(2) Animal experiments

Prior to the measurement, the myocardial assist device was installed in the thoracic cavity and anchored onto the surface girdling the heart by under general anesthetising procedure. The hemodynamic waveforms were obtained from healthy goats, the mean weight of which was 53 kg. Pulmonary and aortic blood pressures were measured by transducers and amplified with a polygraph (Fukuda Denshi, MCS-5000). The aortic flow rate was also measured at the aortic root by an ultrasonic flowmeter (Transonic Systems, TS420). Each data was digitally recorded with a data recorder (TEAC, LX-10) by the sampling frequency of 1.5 kHz.

All the animal experiments related to this study were scrutinised and approved by the Ethical Committee on Animal Experiments of the Department of Medicine, Tohoku University, and also the Institute of Development, Aging and Cancer, Tohoku University, 2004–2006.

### 3. Results and Discussion

Figure 5 shows the transient response of the Biometal fibre under the different input conditions. The duty ratio was changed from 50 to 300msec, and there was no discernible variation of the speed of the stress gain. As the actuation was conducted only by the cooling-and-heating process in the fibre, neither a sound nor an electric noise could be easily generated in each part.

The myocardial device developed was successfully installed into the goats' thoracic cavity. Prior to the installation of the device, it was covered with silicone rubber

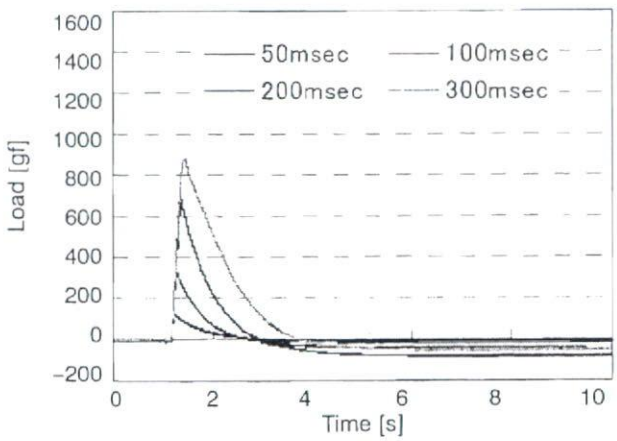


**Fig. 5.** Basic characteristics of the transient response obtained from a single fibred module under the different pulse wave modulation input conditions; the duty of the input was set to be 50, 100, 200, 300 msec respectively at the room temperature (25°C)

and PVC polymer. For the installation of the former electrohydraulic myocardial assist device, which was developed by the authors [6], it was necessary to remove at least the fifth costa to make enough room to fit it into the thoracic cavity. But in this study, by using shape memory fibres, the actuator itself was so small that it would require even a smaller volume in the thoracic cavity. Moreover, the procedure of the closed chest was found to be much simpler. However, any other complications which might have been associated with the operation were not confirmed in goats yet.

Hemodynamic waveforms were changed by the mechanical assistance as shown in Fig. 6. The aortic flow rate was increased by 23% and the systolic left ventricular pressure was elevated by 6% under the low cardiac output condition at 2.5 l/min by the mechanical assistance. Therefore, it was indicative of the point that the effective assistance might have been achieved by using those shape-memory alloy fibres.

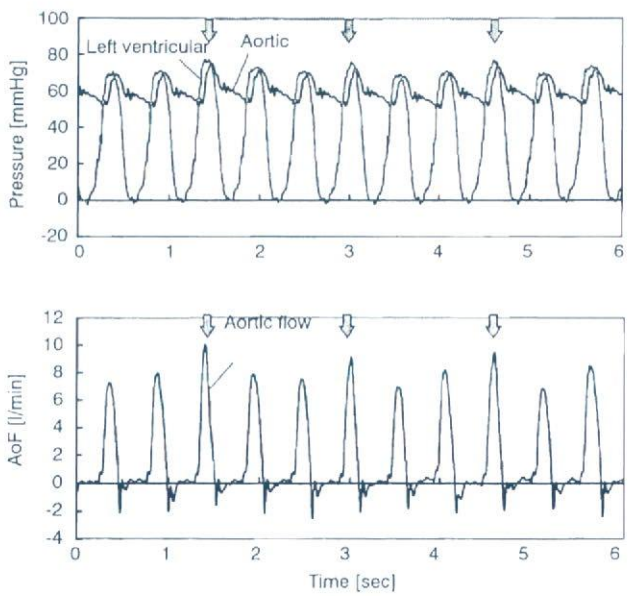


**Fig. 6.** Changes in hemodynamic waveforms obtained in a goat; the arrows indicated the mechanical contractile assistance by the artificial myocardial developed. The assistance was carried out one third of the natural heart beat

## 4. Conclusion

The newly-designed mechano-electric artificial myo-cardium was developed by using a shape memory alloy fibre, which was capable to be totally installed into the thoracic cavity. It was easy to attach the device onto the ventricular wall. And also

the preliminary examination of the performance of the device was conducted in goat experiments. The amelioration of the cardiac functions following the changes in the vascular hemodynamics were investigated by the mechanical assist. As our system could be a symbiotic autonomous system which is capable of assisting natural ventricular functions with physiological deficit, it might be useful for the application in patients with chronic heart failure, such as angina of effort, and also as the cardiac massage in life-saving emergency for the recovery from ventricular fibrillation, as an alternative circulatory support.

**Acknowledgments**

The authors would like to extend their appreciation to Mr. Kimio Kikuchi and Mr. Tomio Kumagai for their cooperation in the animal experiments. This study was supported by Grant in Aid for Scientific Research of Ministry of Health, Labour and Welfare (H17-nano-009), and Ministry of Education, Culture, Sports, Science and Technology (17790938). And this study was partly supported by Grant in Aid for Scientific Research of Pharmaceuticals and Medical Devices Agency (02-1).

## References

1. Hosenpud J.D., et al.: The registry of the international society for heart and lung transplantation: fifteenth offi-cial report–1998, J. Heart Lung Transplant., 1998, 17, 656–668.
2. Shimizu T., et al.: Fabrication of pulsatile cardiac tissue grafts using a novel 3-dimensional cell sheet manipulation technique and temperature-responsive cell culture surfaces, Circ. Res., 2002, 90(3), e40.
3. Nitta S., et al.: Application of shape memory alloy for an artificial heart driving system, MBE 1983, 83–49, 45–51 (in Japanese).
4. Yambe T., et al.: Addition of rhythm to non-pulsatile circulation, Biomed. Pharmacother., 2004, 58, Suppl. 1, S145-9.
5. Yambe T., et al.: Artificial myocardium with an artificial baroreflex system using nano technology, Biomed. Pharmacother., 2004, 57 Suppl. 1, 122–125.
6. Wang Q., et al.. An artificial myocardium assist system: electrohydraulic ventricular actuation improves myocardial tissue perfusion in goats, Artif. Organs, 2004, 28(9), 853–857.
7. Andtadt G.L., et al.: A new instrument for prolonged mechanical massage, Circulation, 1965, 31 (Suppl. II), 43.
8. Anstadt M., et al.: Direct mechanical ventricular actruator, Resuscitation, 1991, 21, 7–23.
9. Kawaguchi O., et al.: Dynamic cardiac compression improves contractile efficiency of the heart, J. Thorac. Cardiovasc. Surg., 1997, 113, 923–931.
10. Buehler W.J., Gilfrich J., Wiley K.C.: Effect of low-temperature phase changes on the mechanical properties of alloys near composition TiNi, J. Appl. Phys., 1963, 34, 1465.
11. Homma D., Miwa Y., Iguchi N., et al.: Shape memory effect in Ti-Ni alloy during rapid heating, Proc. of 25th Japan Congress on Materials Research, 1982.
12. Sawyer P.N., et al.: Further study of NITINOL wire as contrctile artificial muscle for an artificial heart, Carrdiovasc. Diseases Bull. Texas Heart Inst., 1976, 3, 65.
13. Westerby S.: Non-transplant surgery for heart failure, Heart, 83, 2000, 603–610.
14. Suma H., et al.: Non transplant cardiac surgery for end-stage cardiomyopathy, J. Thorac. Cardiovasc. Surg., 2000, 119, 1233–1244.

15. Raman J.S., et al.: The mid-term results of ventricular containment (Acorn Wrap) for end-stage ischemic cardiomyopathy, 2005.
16. Pilla J.J., et al.: Ventricular constraint using the cardiac support device reduces myocardial akinetic area in an ovine model of acute infarction, Circulation, 2002, 106 [Suppl 1], I207–I211.
17. Uematsu M., Shiraishi Y., et al. Proc. IEEE-EMBS, 2005.

# Mechanical integrative design for sophisticated artificial myocardial contraction

Yasuyuki Shiraishi[1], Tomoyuki Yambe[1], Yoshifumi Saijo[1], Muneichi Shibata[1], Tasuku Yamaguchi[1], Ken Matsue[1], Hongjian Liu[1], Atsushi Baba[2], Kou Imachi[2], Hiroshi Sasada[3], Yumiko Wada[4], Ryo Sakata[4], Tomoki Watabe[4], Hui Lin[4], Mitsuo Umezu[4], Koichi Tabayashi[5], and Dai Homma[6]

1) Institute of Development, Aging and Cancer, Tohoku University
2) Tohoku University Biomedical Engineering Research Organization (TUBERO), Tohoku University
3) Graduate School of Agriculture, Tohoku University
4) Graduate School of Science and Engineering, Waseda University
5) Graduate School of Medicine, Tohoku University
6) Toki Corporation
E-mail: shiraishi@idac.tohoku.ac.jp

## Abstract

The authors have been developing an artificial myocardium by using a covalent-type shape memory alloy fibre, which is capable of supporting ventricular contractile function in each severe heart failure patient. In order to improve its effective assistance from outside of the heart, the anatomical myocardial structure in a goat's heart had been scanned by CT, and the oblique design of the artificial myocardial assist device was reproduced which was to represent native cardiac construction. And the cardiac wall-thickening effect was mechanically simulated by using hinge structures which were connected sequentially. Basic characteristics and hemodynamic effects of the circumferential or oblique types were examined in goat experiments (n=4) as well as in the mock circulatory system. The results were as follows: a) In the hydrodynamic test using the mock circulatory system, the volume assisted which was elevated by 39% by morphological design, b) Hemodynamic data obtained in goats indicated the more effective volumetric assistance by the oblique design. Therefore, it was suggested that the morphological design of artificial myocardial support system could be more effective for the functional improvement of artificial myocardium as well as its control system design.

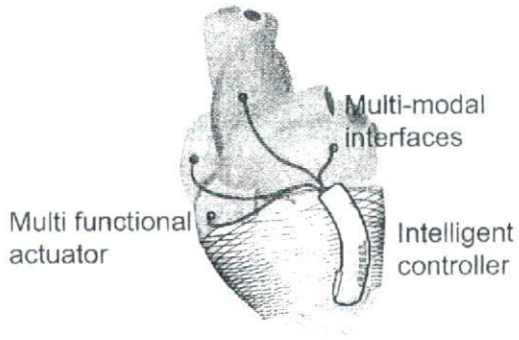


Fig. 1. Schematic illustration of a concept for the sophisticated mechanical contractile assistance by using the artificial myocardium with shape memory alloy fibre (upper), and the special features of the covalent structured shape memory alloy material (bottom).

## 1. Introduction

In general, patients with the end stage of severe heart failure, who present an increased ventricular filling pressure or insufficient amount of blood supply to organs, are given medical or surgical treatment. Recently, artificial circulatory assistance by using ventricular assist devices, such as artificial hearts, has been provided, which is followed by heart transplantation. However, the deficiency of donor hearts might be a serious problem in the world. And the transplantation waiting period in this country extends to several years [1]. Therefore, necessity of clinical application of artificial hearts with long-term durability has arisen. As the size of the western ventricular assist devices, which are provided at present, is still big for the smaller body size Asian people, several artificial

heart projects are being conducted in Japan, and one of these has started clinical trials.

There are also some devices or procedures suggested to be useful for the surgical treatment of severe heart failure, such as the ventricular CorCup or Myosplint. However, those procedure for the surgical treatment might not provide the active contractile assistance for diseased heart although the diastolic dilatation could be chronically and statically prevented [2-5].

As the heart failure is caused by a lessening of myocardial contractile tension, the direct mechanical myocardial assistance in response to physiological deficit, i.e. a synchronous support of the contractile function from outside of the heart, might be effective. The purpose of this study was to develop an artificial myocardium, which would be capable of supporting the cardiac contraction directly by using the shape memory alloy fibre of a minute diameter around 100um based on nanotechnology.

The authors have been developing a totally-implantable artificial myocardial assist device [6-10]. In this study, the authors fabricated a newly-designed oblique structure and wall-thickening components for contraction by using our shape memory alloy fibred myocardial assist device, and examined thier hydrodynamic or hemodynamic functions in the originally-designed mock circulatory system as well as in goats.

## 2. Methods

### 2.1. Anatomical structures of the heart

In order to investigate the native anatomical myocardial structure, a goat' heart was unfolded in accordance with Torrent-Guasp's theory [11,12] as shown in Figure 2. Myocardial streamlines from the apex to aortic root could be investigated by the removal of the right ventricular wall, and its angle against the longitudinal axis of the left ventricle seemed to be around 40-45 degree.

And also the three-dimensional figure had been reconstructed by the computed tomography (Siemens, Somato Definition) as shown in Figure 3. Then inner layered structure and myocardial streamlines of the heart could be investigated.

### 2.2. Angular and oblique design of the myocardial assist device

Based on the measurement of anatomical structure of the heart, an angular and an oblique shape types of myocardial assist device, which would be able to girdle the ventricle along with the myocardial streamlines, were fabricated as shown in Figure 4. In the angular type, two components of the shape memory alloy band were connected, and the direction of each component was set to be parallel with myocardial streamlines. And in the oblique type, the band was straight shaped along with the parallel-linked shape memory alloy fibres.

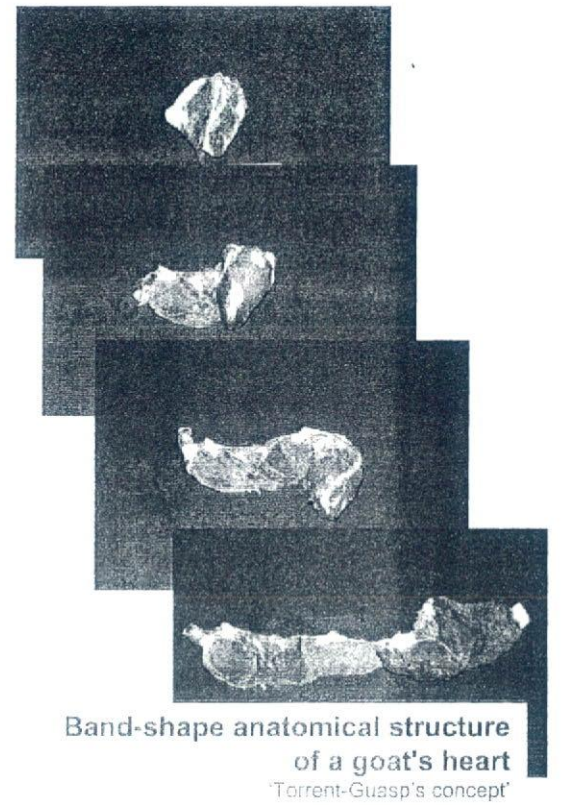


(a) Sequential representation of the myocardial structure unfolded of a goat heart.

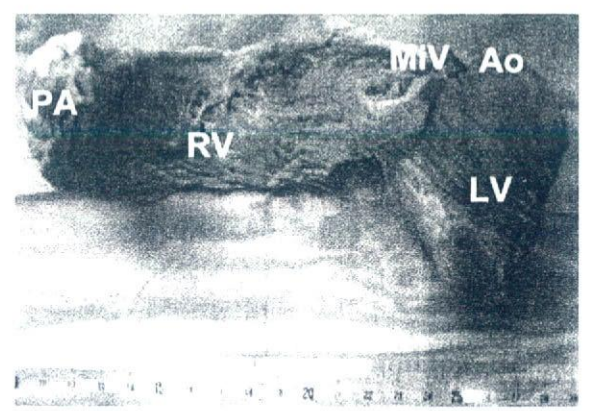


(b) An unfolded portion of the left ventricle treated by formalin-fixation; myocardial tissue streamline for the morphologic spatial configuration could be investigated at the 'LV' portion

Fig. 2. Band –shape anatomical structure of a goat heart unfolded according to Torrent-Guasp's anatomical concept.

### 2.3. Built-in 'solid' truss implementation in the device

For more sophisticated representation of native cardiac contraction as shown in Figure 5, as well as the effective magnification of contractile volumetric assistance, a built-in truss mechanism had been implemented on the artificial myocardial band (Figure 6). And its performance was also examined in the mock circulatory system simulating the normal systemic circulatory afterload.

## 3. Results and Discussion

### 3.1. Hydrodynamic and hemodynamic effects of different types of myocardial assist device

The oblique design of the myocardial assist device was made to form the contractile streamlines from the apex to ascending aorta. Basic characteristics and hemodynamic effects of the circumferential or oblique types were examined in goat experiments (n=4) as well as in the mock circulatory system. The results were as follows:

a) In the hydrodynamic test using the mock circulatory system, the volume assisted which was elevated by 39% by morphological design.

b) Hemodynamic data obtained in goats indicated the more effective volumetric assistance by the oblique design, and on the other hand there was no significant difference in systolic assisted pressure.

Therefore, it was suggested that the morphological design of artificial myocardial support system could be more effective for the functional improvement of artificial myocardium as well as its control system design.

### 3.2. Hydrodynamic changes by built-in hinge mechanism

In the hydrodynamic test, the aortic forwarded flow rate was increased by 20% (from 2.8 to 3.4 L/min) against 75mmHg afterload by the 'solid' hinge mechanism implemented. And the ventricular pressure which was measured in the silicone left ventricular model was also elevated by 12%.

## 4. Conclusion

The mechano-electric myocardium was developed and improved by mechanical integrated design by using shape memory alloy fibres. The device was able to be totally installed into the goat's thoracic cavity. The amelioration of the cardiac functions following the changes in the vascular hemodynamics were investigated by the mechanical assist. As our system could be a symbiotic autonomous system which is capable of assisting natural ventricular functions with physiological deficit, it might be useful for the

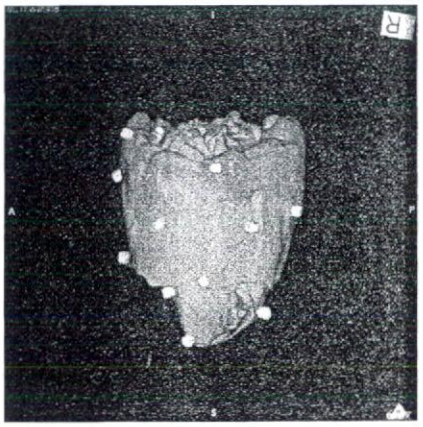

Fig. 3. Numerical reconstruction of the goat's heart from the data measured by MDCT; the white-coloured plastic markers indicated the centre and the edges at each portion of myocardial band unfolded.

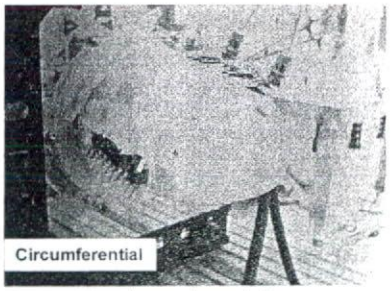


(a) circumferential-type

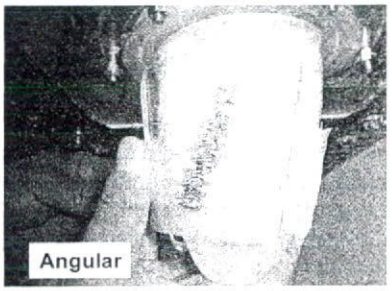


(b) angular-type

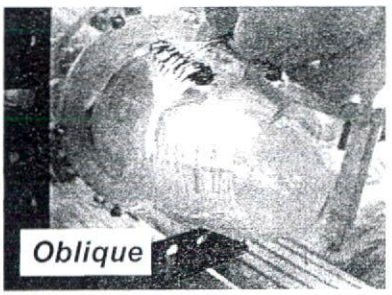


(c) oblique-type

Fig. 4. Three different types of prototype models for the artificial myocardial support, which were attached on the silicone left ventricular model.

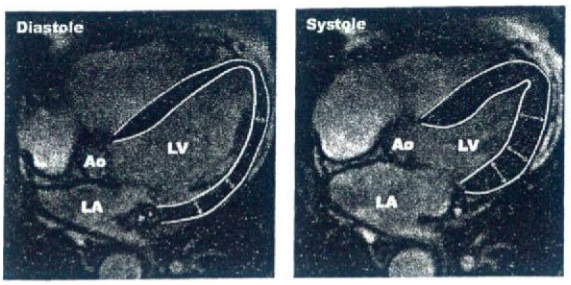


Fig. 5. Normal cardiac contraction and wall-thickening effect obtained at a healthy subject by MRI.

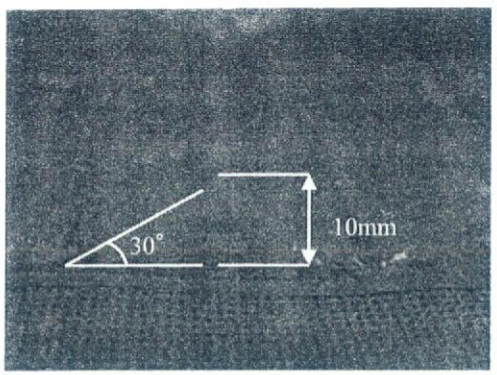


Fig. 6. Newly-designed built-in 'solid' hinge implemented in the myocardial assist device.

application in patients with chronic heart failure such as angina of effort, and also as the cardiac massage in life-saving emergency for the recovery from ventricular fibrillation, as an alternative circulatory support. And its flexible and self-contractile functions might be also useful for the cardiac functional support as well as the treatment of severe ischemic heart failure, such as ventricular aneurysm, which is primarily treated by surgical ventricular restoration.

All the animal experiments related to this study were investigated and approved by the Ethical Committee on Animal Experiments of Graduate School of Medicine, Tohoku University, and also of the Institute of Development, Aging and Cancer, Tohoku University, 2004-2007.

## Acknowledgements

The authors would like to extend their appreciation to Mr. K. Kikuchi and Mr. T. Kumagai for their cooperation in the animal experiments. This study was supported by Grand in Aid for Scientific Research of Ministry of Health, Labour and Welfare (H17-nano-009), and Ministry of Education, Culture, Sports, Science and Technology (17790938, 19689029).

## References

[1] Taylor TD, et al. Registry of the International Society for Heart and Lung Transplantation: Twenty-fourth Official Adult Heart Transplant Report—2007. *J Heart Lung Transplant* **26**(8), 769-781, 2007.
[2] Anstadt GL, et al. A new instrument for prolonged mechanical massage, *Circulation* **31**(Suppl.II), 43, 1965.
[3] Anstadt M, et al. Direct mechanical ventricular actuator, *Resuscitation* **21**, 7-23, 1991.
[4] Power JM, et al. Efficacy of the Acorn cardiac support device in animals with heart failure secondary to high rate pacing, *Heart Failure Reviews* **10**, 117-123, 2005.
[5] McCarthy PM, et al. Device-based change in left ventricular shape: A new concept for the treatment of dilated cardiomyopathy, *JTCS* **122**(3), 482-290, 2001.
[6] Nitta S, et al. Application of shape memory alloy for an artificial heart driving system. *MBE* **83-49**, 45-51, 1983 (in Japanese).
[7] Yambe T, et al. Addition of rhythm to non-pulsatile circulation. *Biomed Pharmacother* **58**(Suppl.1), S145-9, 2004.
[8] Yambe T, et al. Artificial myocardium with an artificial baroreflex system using nanotechnology. *Biomed Pharmacother* **57**(Suppl.1), S122-5, 2004.
[9] Wang Q, et al. An artificial myocardium assist system: electrohydraulic ventricular actuation improves myocardial tissue perfusion in goats. *Artif Organs* **28**(9), 853-7, 2004.
[10] Shiraishi Y, et al. A newly-designed myocardial assist device using a sophisticated shape memory alloy fibre, *Biocyber and Biomed Eng* **27**(1/2), 147-154, 2007.
[11] Corno AF, et al. The helical ventricular myocardial band of Torrent-Guasp: potential implications in congenital heart defects, *EJCTS* **29S**, S61-S68, 2006.
[12] Torrent-Guasp F, et al. Spatial orientation of the ventricular muscle band – physiologic contribution and surgical implications, *JTCS* **122**, 389-92, 2001.
[13] Buehler WJ, et al. Effect of low-temperature phase changes on the mechanical properties of alloys near composition TiNi, *J Appl Phys* **34**, 1465, 1963.
[14] Homma D, et al. Shape memory effect in Ti-Ni alloy during rapid heating, *Proc 25th Japan Congress on Materials Res*, 1982.
[15] Westerby S. Non-transplant surgery for heart failure. *Heart* **83**, 603-610, 2000.

*The American Journal of Pathology, Vol. 171, No. 4, October 2007*

*DOI: 10.2353/ajpath.2007.061191*

*Cardiovascular, Pulmonary and Renal Pathology*

# Macrophage Colony-Stimulating Factor Improves Cardiac Function after Ischemic Injury by Inducing Vascular Endothelial Growth Factor Production and Survival of Cardiomyocytes

Tatsuma Okazaki,* Satoru Ebihara,* Masanori Asada,* Shinsuke Yamanda,* Yoshifumi Saijo,† Yasuyuki Shiraishi,† Takae Ebihara,* Kaijun Niu,* He Mei,* Hiroyuki Arai,* and Tomoyuki Yambe†

*From the Department of Geriatrics and Gerontology,* Tohoku University School of Medicine, Sendai; and the Department of Medical Engineering and Cardiology,† Institute of Development, Aging, and Cancer, Tohoku University, Sendai, Japan*

**Macrophage colony-stimulating factor (M-CSF), known as a hematopoietic growth factor, induces vascular endothelial growth factor (VEGF) production from skeletal muscles. However, the effects of M-CSF on cardiomyocytes have not been reported. Here, we show M-CSF increases VEGF production from cardiomyocytes, protects cardiomyocytes and myotubes from cell death, and improves cardiac function after ischemic injury. In mice, M-CSF increased VEGF production in hearts and in freshly isolated cardiomyocytes, which showed M-CSF receptor expression. In rat cell line H9c2 cardiomyocytes and myotubes, M-CSF induced VEGF production via the Akt signaling pathway, and M-CSF pretreatment protected these cells from $H_2O_2$-induced cell death. M-CSF activated Akt and extracellular signal-regulated kinase signaling pathways and up-regulated downstream anti-apoptotic Bcl-xL expression in these cells. Using goats as a large animal model of myocardial infarction, we found that M-CSF treatment after the onset of myocardial infarction by permanent coronary artery ligation promoted angiogenesis in ischemic hearts but did not reduce the infarct area. M-CSF pretreatment of the goat myocardial infarction model by coronary artery occlusion-reperfusion improved cardiac function, as assessed by hemodynamic parameters and echocardiography. These results suggest M-CSF might be a novel therapeutic agent for ischemic heart disease.** ***(Am J Pathol 2007, 171:1093–1103; DOI: 10.2353/ajpath.2007.061191)***

The administration of angiogenic growth factors such as vascular endothelial growth factor (VEGF) is an innovative strategy to treat myocardial ischemia. VEGF has been used in animal models and in clinical trials of myocardial ischemia to develop growth of collateral blood vessels and to promote myocardial perfusion, and its therapeutic potential has been reported.[1–3] Hematopoietic growth factors are potent therapeutic agents for myocardial infarction. Erythropoietin improved cardiac function after myocardial infarction.[4,5] Granulocyte colony-stimulating factor (G-CSF) improved cardiac function and prevented cardiac remodeling after myocardial infarction.[6] A combination of stem cell factor and G-CSF treatment improved cardiac function and survival after myocardial infarction.[7] Macrophage colony-stimulating factor (M-CSF) in combination with G-CSF improved ventricular function after myocardial infarction in rats, but few results were shown by M-CSF treatment alone, and their mechanism was not defined.[8] Moreover, to estimate growth factor-induced therapeutic angiogenesis in hearts, large animal models are necessary,[3] but the effects of M-CSF in large animal models have not been reported. M-CSF has been initially characterized as a hematopoietic growth factor, and has been used to prevent severe infections in myelosuppressed patients after cancer chemotherapy.[9,10] M-CSF stimulates the survival, prolifera-

Supported by the Ministry of Education, Science, and Culture (grants 15590795, 18014004, 17590777, and 18790528); the Ministry of Health, Labor, and Welfare of the Japanese Government (Grant for Longevity Science grants 16C-1 and 18C-7); and by the Program for Promotion of Fundamental Studies in Health Science of Organizing for Drug ADR Relief, R&D Promotion, and Product Review of Japan.

Accepted for publication June 27, 2007

Current address of T.O., Department of Anatomy, University of California–San Francisco, San Francisco, CA.

Address reprint requests to Satoru Ebihara, M.D., Ph.D., Department of Geriatrics and Gerontology, Tohoku University School of Medicine, Seiryo-machi 1-1, Aoba-ku, Sendai 980-8574, Japan. E-mail: s_ebihara@geriat.med.tohoku.ac.jp.

tion, and differentiation of cells from mononuclear phagocyte lineage.[11]

Expression of VEGF in the heart has been documented,[12,13] and cardiomyocytes have been reported as a major source of VEGF in the heart.[12] Skeletal muscles expressed VEGF,[13,14] and M-CSF increased VEGF production from skeletal muscles *in vivo* and *in vitro*,[14] but it is unknown whether M-CSF increases VEGF production from cardiomyocytes. M-CSF treatment increased serum VEGF levels in mice,[14] and the level was in the potentially therapeutic range that could treat ischemic diseases in human patients.[15]

Erythropoietin and G-CSF directly protected cardiomyocytes from cell death stimulation.[4,6] M-CSF improves the survival of mononuclear phagocyte lineage cells,[11] but the cell survival effect of M-CSF on cardiomyocytes is unknown. As for their signaling pathways, M-CSF activates Akt, extracellular signal-regulated kinase (ERK), and/or Janus-associated kinase (Jak)-signal transducer and activator of transcription (STAT) cell signaling pathways in bone marrow-derived macrophages and macrophage cell lines.[16–18] M-CSF increased VEGF production in skeletal muscles via Akt activation *in vitro*.[14] However, the cell signaling pathways of M-CSF in cardiomyocytes have not been investigated.

In the present study, we investigated the angiogenic and protective effects of M-CSF on cardiomyocytes *in vitro* and *in vivo*, in mice, rats, and goats. We show that M-CSF increases VEGF production in cardiomyocytes via Akt activation, directly protects cultured cardiomyocytes and myotubes from cell death stimulation by Akt and ERK activation and by up-regulation of downstream anti-apoptotic protein Bcl-xL. Moreover, we show the benefits of M-CSF treatment for ischemic heart diseases *in vivo* using goats as a large animal model.

## Materials and Methods

### Reagents and Cell Culture

Human M-CSF (Kyowa Hakko Kogyo, Tokyo, Japan) was dissolved in saline for goat experiments described below or in phosphate-buffered saline (PBS) for other experiments. Phycoerythrin-labeled anti-M-CSF receptor (M-CSF-R) monoclonal antibody, control rat IgG2a, and unlabeled anti-CD16/32 monoclonal antibody were purchased from eBioscience (San Diego, CA). H9c2 cells (American Type Culture Collection, Manassas, VA) were cultured in high-glucose Dulbecco's modified Eagle's medium containing 10% fetal calf serum, 100 U/ml penicillin, and 0.1 mg/ml streptomycin (growth medium, GM). To induce cardiac differentiation, H9c2 myoblasts were cultured in differentiation medium (DM) with daily supplementation of 10 nmol/L *all-trans*-retinoic acid (ATRA) (Sigma, St. Louis, MO), with medium changed every 2 days.[19] The difference between GM and DM is 1% fetal calf serum in DM. H9c2 myoblasts were differentiated to myotubes by culturing in the same DM for 11 days.[20] Mouse primary cardiomyocytes were obtained from 1- to 3-day-old neonatal C57BL/6 mice.[21] Heart ventricles were washed in ice-cold Hanks' balanced salt solution without either $Ca^{2+}$ or $Mg^{2+}$ and then minced. The cells were dissociated with 0.25% trypsin in Hanks' balanced salt solution. The supernatants were collected every 15 minutes and centrifuged. To exclude nonmuscle cells, the cells were cultured at 37°C for 2 hours. Then the suspended cells were collected and cultured at $1 \times 10^5$ cells/cm$^2$. After 48 hours, more than 90% of the cells were considered as cardiomyocytes by cross-striation structure staining with Bodipy FL phallacidin (Molecular Probes, Eugene, OR).

### Cell Proliferation and Cell Death Assays

H9c2 cells ($5 \times 10^3$ cells) were plated on 96-well plates and differentiated to cardiomyocytes or myotubes, and the assays were performed as previously shown.[22] For proliferation assays, H9c2 cardiomyocytes or myotubes were treated with M-CSF for indicated time periods, and the cell numbers were counted by a water-soluble tetrazolium (WST) assay using a cell counting kit (Dojindo, Tokyo, Japan). For cell death assays, differentiated H9c2 cells were incubated with M-CSF in the presence or absence of PD98059 (at 30 or 6 μmol/L; Biosource, Camarillo, CA) or LY294002 (at 10 or 2 μmol/L; Biosource) for 24 hours. Then the cells were stimulated with indicated amount of $H_2O_2$ for 8 hours. The cell viability was determined by the WST assay.

### Flow Cytometry

The cells were incubated with unlabeled anti-CD16/32 monoclonal antibody to block nonspecific binding and then with phycoerythrin-labeled antibodies. Flow cytometry was performed with a FACScan (BD Bioscience, San Jose, CA).[14]

### Histology

The goat hearts were fixed in 10% formalin, embedded in paraffin, and sectioned. The sections were stained with hematoxylin and eosin (H&E) or Masson's elastic stain. The microvessel density in myocardial infarction lesions was determined as previously shown by immunohistochemical staining of goat hearts with polyclonal rabbit anti-human factor VIII-related antigen antibody (DakoCytomation, Carpinteria, CA) at 1:200 dilution.[14,23] The applicability of this antibody to goats was previously reported.[24] The image with the highest microvessel density was chosen at ×100 magnification, and the vessels were counted at ×200 magnification. Two independent investigators counted at least four fields for each section, and the highest count was taken. To quantify the infarct area, a standard point-counting technique was used as previously described with minor modifications.[25] In brief, the whole heart cross section with highest infarct area was selected, and a 200-point grid was superimposed onto each captured image using Adobe Photoshop (Adobe Systems Inc., San Jose, CA). The area fraction of infarction was

calculated by dividing the number of infarct points by the total number of points falling on the tissue section and was expressed as a percentage.

### *Western Blot Analysis*

Western blot analysis was performed as shown previously.[26] H9c2 myoblasts ($5 \times 10^6$ cells) were cultured in GM on day 0. From day 1, the cells were differentiated to cardiomyocytes or myotubes. After differentiation, the cells were serum-starved for 6 hours and stimulated with M-CSF. For inhibitor experiments, the cells were cultured with inhibitors for 30 minutes and then stimulated with M-CSF and inhibitors. PD98059 was incubated at a concentration of 30 or 6 $\mu$mol/L, and LY294002 was incubated at a concentration of 10 or 2 $\mu$mol/L. The cell lysates were subjected to 12% sodium dodecyl sulfate-polyacrylamide gel electrophoresis and transferred onto polyvinylidene difluoride membranes (Millipore, Billerica, MA). The membranes were blotted with antibodies to phospho-ERK, phospho-Akt, phospho-Stat1, phospho-Stat3, phospho-Bad, Bcl-xL (Cell Signaling Technology, Beverly, MA), phospho-Jak1, or M-CSF-R (Santa Cruz Biotechnology, Santa Cruz, CA). The membranes blotted with antibodies to detect phosphorylation were then reblotted with antibodies to total ERK, Akt, Stat1, Stat3, Bad (Cell Signaling Technology), or Jak1 (Santa Cruz Biotechnology).

### *Mouse and Goat Preparation*

The Laboratory Animal Committee at Tohoku University approved all animal experiments. Male C57BL/6 mice, 7 to 9 weeks old, were injected intramuscularly with M-CSF (200 $\mu$g/kg body weight) or PBS (control) for 3 consecutive days ($n = 5$ per group). Adult male goats (48 to 53 kg body weight) were intubated and anesthetized with 2% halothane as previously reported ($n = 3$ per group).[27] The goats were incised between the fourth and fifth ribs, and a left lateral thoracotomy was performed. Myocardial infarction was induced by left anterior descending coronary artery ligation with some modifications.[28] For the permanent left anterior descending coronary artery ligation model, left anterior descending coronary artery was ligated at a point ~60% from the beginning of the left coronary artery to the apex. M-CSF (40 $\mu$g/kg body weight) intravenous injection began just after the ligation and continued daily for 13 days; on day 14, the goats were anesthetized with 2% halothane and sacrificed. Control goats were injected with saline. For the ischemia-reperfusion model, M-CSF was injected intravenously for 3 consecutive days. Then the left anterior descending coronary artery was ligated at a point ~40% from the beginning of the left coronary artery to the apex for 30 minutes followed by reperfusion.[5] A micromanometer tipped catheter (Millar Instruments Inc., Houston, TX) was positioned in the left ventricle (LV). Hemodynamic parameters were recorded using a data recording unit (TEAC Corp., Tokyo, Japan) with sampling frequency of 1.5 kHz. Echocardiography was performed using a Sonos 5500 (Hewlett Packard, Andover, MA).

### *Enzyme-Linked Immunosorbent Assay (ELISA)*

Mouse hearts were isolated, washed, homogenized in ice-cold PBS, and centrifuged. The protein level in the supernatant was adjusted to 10 mg/ml by the BCA protein assay kit (Pierce, Rockford, IL), and subjected to ELISA using a VEGF ELISA kit (R&D Systems, Minneapolis, MN). Carrageenan (Sigma) and rat anti-mouse CD11b monoclonal antibody (Serotec, Oxford, UK) treatment was performed as previously reported.[14] Culture medium of mouse primary cardiomyocytes ($2 \times 10^5$ cells) was changed daily. H9c2 myoblasts ($5 \times 10^3$ cells) were differentiated to cardiomyocytes or myotubes. H9c2 cardiomyocytes were incubated with M-CSF and ATRA in the presence or absence of LY294002 (10 $\mu$mol/L) for indicated time periods with daily culture medium change. H9c2 myotubes were cultured with M-CSF for indicated time periods. All of the supernatants were assayed by ELISA.

### *RNA Isolation and Reverse Transcriptase-Polymerase Chain Reaction (RT-PCR)*

Total RNA was isolated using RNAzol B reagent (Tel-Test, Friendswood, TX). Placenta total RNA was purchased from BD Biosciences. Quantitative RT-PCR for VEGF and conventional RT-PCR for M-CSF-R were performed as previously shown.[14]

### *Data Analysis*

Data are presented as mean ± SD. Statistical analysis was performed using analysis of variance with Fisher's least significant difference test. $P$ values $<0.05$ were considered as significant.

## *Results*

### *M-CSF Increases Heart VEGF Production* in Vivo

Previous studies have shown that M-CSF increased VEGF production in skeletal muscles, and the heart expresses VEGF. Therefore, we examined whether M-CSF increases heart VEGF production. Mice were treated with M-CSF, and then the cytoplasmic RNA in heart was assessed by quantitative RT-PCR. M-CSF significantly increased VEGF mRNA expression level in the hearts by 221% (Figure 1A). M-CSF receptor (M-CSF-R) mRNA expression was confirmed by conventional RT-PCR, and placenta-derived mRNA was used as a positive control (Figure 1B). To confirm VEGF at the protein level, M-CSF was injected into mice. The hearts were isolated, and ELISA for VEGF was performed. VEGF was detected in controls (Figure 1C). M-CSF significantly increased VEGF in the hearts by 21% (Figure 1C). Because M-CSF induces VEGF production *in vitro* from human monocytes,[29] we sought to clarify whether cardiomyocytes or the monocytes/macrophages in the heart produced VEGF after M-CSF treatment. Mice were treated with carra-

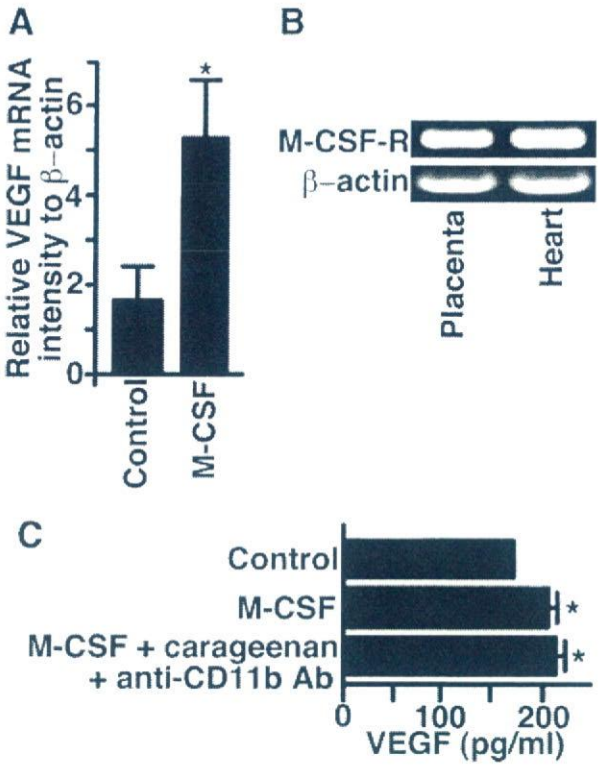


**Figure 1.** M-CSF increased heart VEGF production *in vivo*. Mice were injected intramuscularly with M-CSF (200 μg/kg) or PBS (control) for 3 consecutive days ($n = 5$ per group). **A:** Quantitative RT-PCR determined the VEGF mRNA expression. M-CSF treatment significantly increased the VEGF mRNA expression in hearts ($^*P < 0.05$). **B:** Conventional RT-PCR determined the M-CSF receptor (M-CSF-R) expression (top), and β-actin expression (bottom). **C:** The hearts were washed, homogenized in PBS, and centrifuged. ELISA determined the VEGF level in the supernatants containing 10 mg/ml protein. M-CSF significantly increased the VEGF level. M-CSF + carrageenan + anti-CD11b Ab indicates mice injected with carrageenin (1 mg) on days 1 and 4, with anti-CD11b monoclonal antibody (0.5 mg) on days 3 and 5, and with M-CSF on days 3, 4, and 5. On day 6, the hearts were isolated. This treatment did not affect the VEGF level ($^*P < 0.05$). Similar results were obtained from two independent experiments.

geenan and anti-CD11b monoclonal antibody to eliminate the monocytes/macrophages, as shown previously.[14] Macrophages were hardly observed in control mice hearts or in treated mice hearts (data not shown). The treatment did not affect M-CSF-induced VEGF production in the heart (Figure 1C).

## *M-CSF Increases VEGF Production by Cardiomyocytes* in Vitro

To confirm the effect of M-CSF on heart VEGF production *in vitro*, mouse neonatal cardiomyocytes were isolated and stimulated with M-CSF. The culture medium was changed daily to maintain cell viability. Control cardiomyocytes produced VEGF, and M-CSF significantly increased the VEGF level on days 2 (by 10%) and 3 (by 31%) (Figure 2A). The M-CSF-R expression on cardiomyocytes was confirmed by fluorescence-activated cell sorting analysis (Figure 2B).

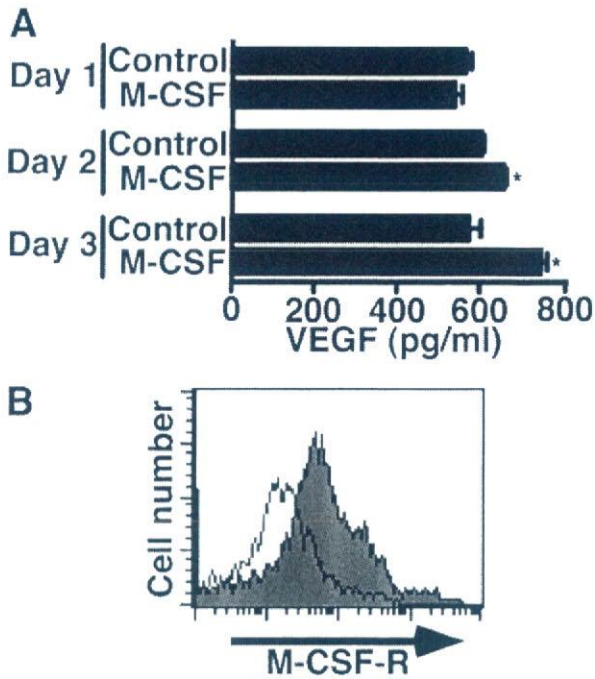


**Figure 2.** M-CSF enhanced heart VEGF production *in vitro*. **A:** Cultured cardiomyocytes from neonatal mice were stimulated with M-CSF (100 ng/ml) for the indicated time periods. Culture medium was changed daily, and the supernatants were subjected to ELISA. M-CSF significantly enhanced VEGF production on days 2 and 3 ($^*P < 0.01$). **B:** Cultured cardiomyocytes from neonatal mice expressed M-CSF-R. The shaded histogram indicates staining with M-CSF-R, and the blank histogram indicates background staining with control IgG. Similar results were obtained from two independent experiments.

## *M-CSF Increases VEGF Production from Differentiated H9c2 Cells*

To investigate the effects of M-CSF on cardiomyocytes more precisely, rat H9c2 myoblast cells were differentiated to cardiomyocytes. H9c2 myoblasts differentiate to cardiomyocytes when they are cultured in DM with ATRA.[19] After differentiation, DM with ATRA was changed daily to maintain cell viability. VEGF was detected in supernatants from controls, and M-CSF increased H9c2 cardiomyocyte VEGF production on days 2 (by 10%) and 3 (by 20%) (Figure 3A). M-CSF increased skeletal muscle VEGF production.[14] H9c2 myoblasts cultured in the DM without ATRA for 11 days differentiate to H9c2 myotubes.[20] After differentiation, H9c2 myotubes were treated with M-CSF. H9c2 myotubes produced VEGF, and M-CSF significantly enhanced VEGF production on day 8 by 29% (Figure 3B).

## *M-CSF Protects Differentiated H9c2 Cells from $H_2O_2$-Induced Cell Death*

Because M-CSF increased VEGF production from differentiated H9c2 cells, we investigated whether M-CSF increased the H9c2 cardiomyocyte cell number and found that it did not (Figure 4A). Similar results were obtained from the H9c2 myotubes (Figure 4A). M-CSF improves the survival of the mononuclear phagocyte lineage

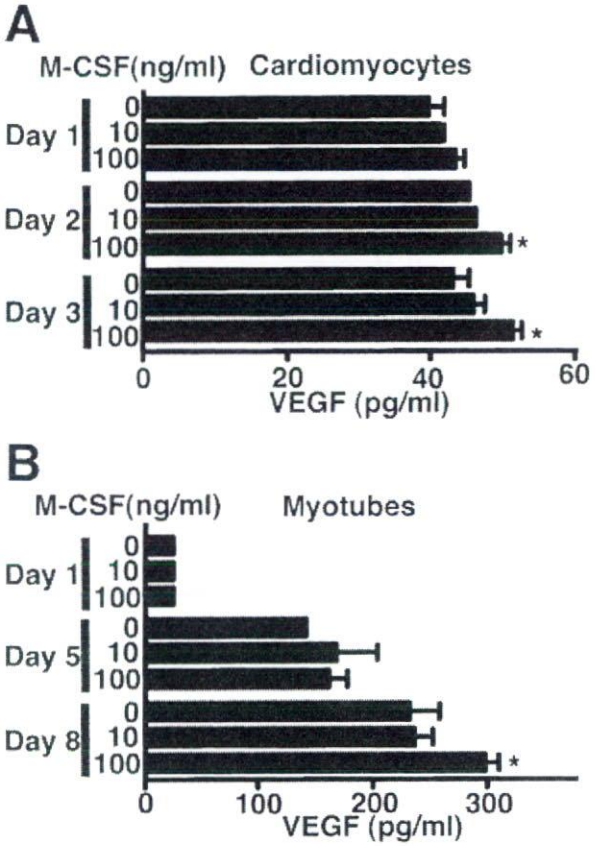


**Figure 3.** M-CSF increased VEGF production in differentiated H9c2 cells. **A:** H9c2 myoblasts cultured in DM (changed every 2 days) with daily supplementation of 10 nmol/L ATRA for 7 days were differentiated to H9c2 cardiomyocytes. The cells were stimulated with the indicated amount of M-CSF for indicated time periods. The culture medium was changed daily, and ELISA determined the VEGF level in the supernatant. M-CSF (100 ng/ml) increased VEGF production on days 2 and 3 ($^*P < 0.05$). **B:** H9c2 myoblasts cultured in the same DM for 11 days were differentiated to H9c2 myotubes. Then the cells were stimulated with the indicated amount of M-CSF for the indicated time periods without medium change. M-CSF (100 ng/ml) significantly increased VEGF production on day 8 ($^*P < 0.03$). Similar results were obtained from three independent experiments.

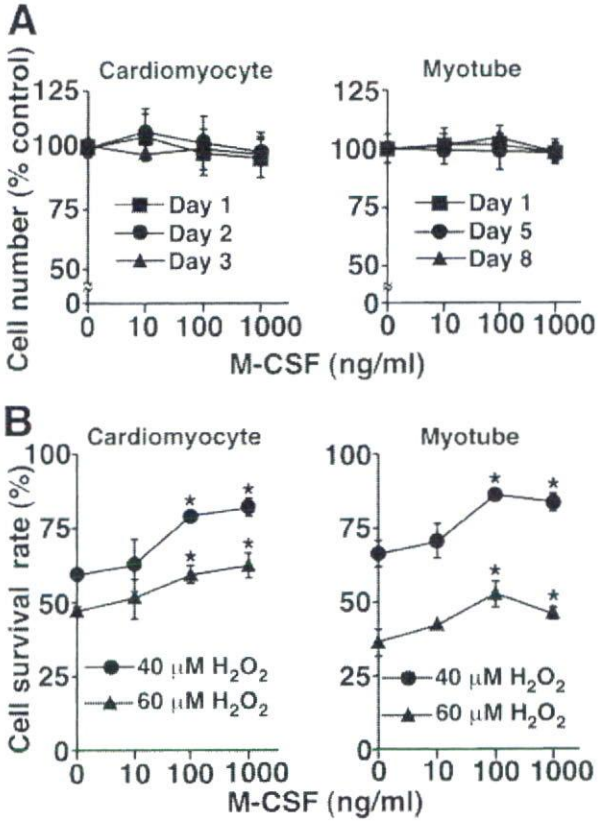


**Figure 4.** M-CSF protects differentiated H9c2 cells from $H_2O_2$-induced cell death. **A:** H9c2 cardiomyocytes were cultured with the indicated amount of M-CSF and ATRA for the indicated time periods, and the culture medium was changed daily. H9c2 myotubes were cultured with the indicated amount of M-CSF for the indicated time periods. WST assay determined the cell number. **B:** H9c2 cardiomyocytes or H9c2 myotubes were cultured with the indicated amount of M-CSF for 24 hours and then stimulated with $H_2O_2$ (40 or 60 μmol/L) for 8 hours. The culture medium of H9c2 cardiomyocytes was supplemented with ATRA. WST assay determined the cell viability. M-CSF (100 and 1000 ng/ml) significantly protected the cells from $H_2O_2$-induced cell death ($^*P < 0.03$). Similar results were obtained from three independent experiments.

cells.[11] Therefore, the cell survival effect of M-CSF on differentiated H9c2 cells from cytotoxic $H_2O_2$ exposure was examined. H9c2 cardiomyocytes were incubated with M-CSF and then exposed to $H_2O_2$. M-CSF significantly protected H9c2 cardiomyocytes from $H_2O_2$-induced cell death (Figure 4B). Similar results were obtained from H9c2 myotubes (Figure 4B).

### *M-CSF Activates ERK and Akt Signaling Pathways and Increases Bcl-xL Expression in Differentiated H9c2 Cells*

The cell signaling pathways of M-CSF in cardiomyocytes and H9c2 myotubes have not been investigated. To elucidate molecular mechanisms of the M-CSF-induced cell survival, differentiated H9c2 cells were treated with M-CSF and then activation of ERK, Akt, and Jak-STAT signaling pathways was investigated. Western blot analysis showed two forms of M-CSF-R in differentiated H9c2 cells (Figure 5, A and C).[30] In H9c2 cardiomyocytes, M-CSF induced ERK activation, as indicated by its protein phosphorylation, whereas the protein levels of the total ERK in cell lysates were not different (Figure 5A). M-CSF activated the Akt, but M-CSF did not activate Jak1, Stat1, or Stat3 (Figure 5A). ERK activation protects cardiomyocytes from cell death by up-regulating the anti-apoptotic protein Bcl-xL and inactivating the apoptotic protein Bad by its phosphorylation at Ser112.[31,32] Akt activation improves cardiomyocyte survival, but the main downstream signaling pathways of Akt for cardiomyocytes survival has not been clarified.[33] To clarify the target molecules of ERK in H9c2 cardiomyocytes, Bcl-xL expression was examined. Bcl-xL was detected in cells without M-CSF stimulation (Figure 5B). M-CSF up-regulated Bcl-xL expression, which peaked at 24 and 48 hours (Figure 5B). M-CSF did not phosphorylate Bad at Ser112 (Figure 5B). These results suggest M-CSF protected H9c2 cardiomyocytes by activating Akt and up-regulating Bcl-xL expression through ERK activation. In H9c2 myotubes, M-CSF activated ERK and Akt but did not activate Jak1 or Stat3

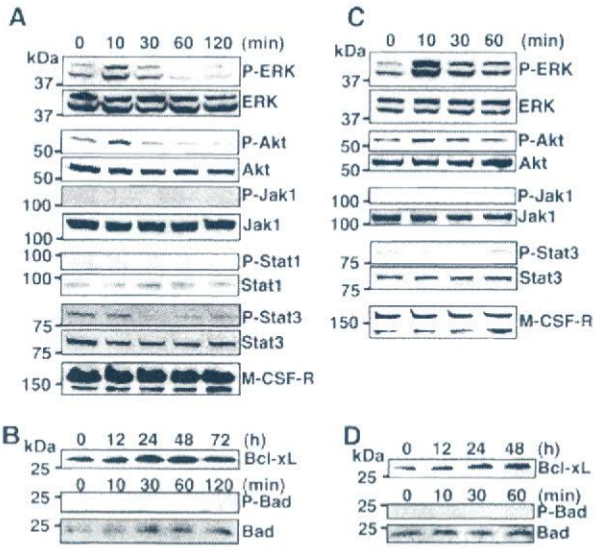


**Figure 5.** M-CSF activated ERK, Akt, and up-regulated Bcl-xL expression in differentiated H9c2 cells. H9c2 cardiomyocytes (**A** and **B**) or H9c2 myotubes (**C** and **D**) were stimulated with M-CSF (100 ng/ml) for the indicated time periods, and then the cell lysates were blotted with antibodies specific for the activated form of ERK (phospho-ERK), Akt (phospho-Akt), Jak1 (phospho-Jak1), Stat1 (phospho-Stat1), Stat3 (phospho-Stat3), or phosphorylated Bad (phospho-Bad). The membranes were reblotted with antibodies to total ERK, Akt, Jak1, Stat1, Stat3, or Bad, respectively. Expression of M-CSF-R or Bcl-xL was confirmed by blotting the membrane with specific antibodies. Similar results were obtained from three independent experiments.

(Figure 5C). M-CSF gradually up-regulated Bcl-xL expression until 48 hours (Figure 5D) but did not phosphorylate Bad at Ser112 (Figure 5D).

## *The Role of M-CSF-Induced Akt and ERK Activation in VEGF Production and Cell Survival in Differentiated H9c2 Cells*

M-CSF increases VEGF production through Akt activation in skeletal muscles. To determine the role of Akt activation in H9c2 cardiomyocytes VEGF production, H9c2 cardiomyocytes were treated with Akt-specific inhibitor LY294002, and the culture supernatant was assayed by ELISA. LY294002 and M-CSF treatment for 2 days significantly impaired VEGF production in H9c2 cardiomyocytes (Figure 6A). LY294002 and M-CSF treatment for 3 days further decreased VEGF production, and the VEGF level became less than the detection level (Figure 6A). To determine the role of ERK and Akt activation after M-CSF treatment in differentiated H9c2 cell survival, differentiated H9c2 cells were treated with LY294002 or the ERK-specific inhibitor PD98059. PD98059 inhibited ERK activation and LY294002 inhibited Akt activation in H9c2 cardiomyocytes (Figure 6B). Similar results were obtained from H9c2 myotubes (data not shown). PD98059 enhanced $H_2O_2$-induced cell death of H9c2 cardiomyocytes (Figure 6C). The protective effect of M-CSF was impaired by PD98059; however, M-CSF significantly protected H9c2 cardiomyocytes from cell death (Figure 6C). A similar result was obtained from LY294002 in H9c2 cardiomyocytes (Figure 6C). In H9c2 myotubes, PD 98059 enhanced $H_2O_2$-induced cell death, and PD98059

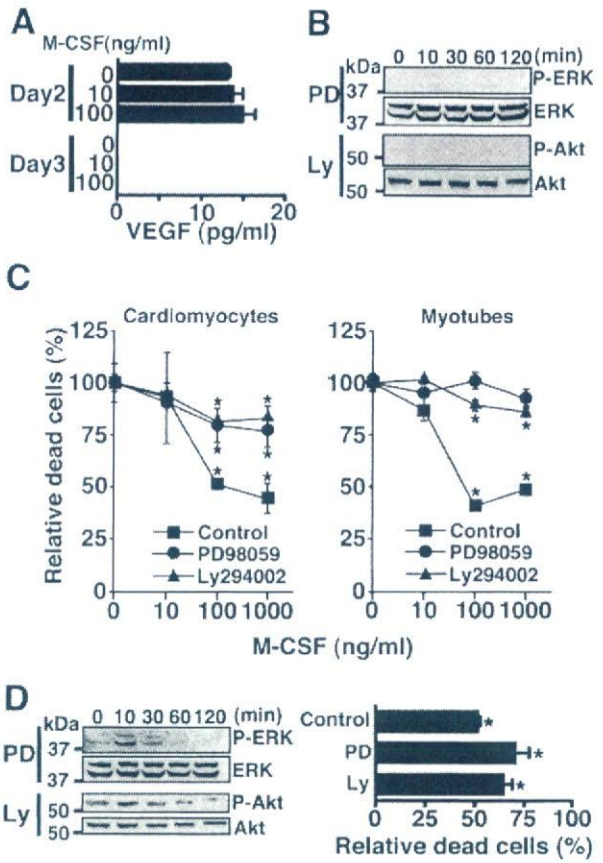


**Figure 6.** The role of M-CSF-induced Akt and ERK activation in VEGF production and cell protection in differentiated H9c2 cells. **A:** H9c2 cardiomyocytes were cultured with M-CSF and 10 μmol/L LY294002 for the indicated time periods. The culture medium was changed daily and ELISA determined the VEGF level. **B:** H9c2 cardiomyocytes were incubated with 30 μmol/L PD98059 (PD) or 10 μmol/L LY294002 (Ly) for 30 minutes, then stimulated with M-CSF (100 ng/ml) and inhibitors, and analyzed as described in Figure 5. **C:** Differentiated H9c2 cells were stimulated with indicated amount of M-CSF with PD98059 (30 μmol/L) or LY294002 (10 μmol/L) for 24 hours. Then the cells were stimulated with $H_2O_2$ (40 μmol/L) for 8 hours, and WST assay determined the dead cells. M-CSF (0 ng/ml) in each group is considered as 100%, and relative cell death rates in each group are shown. $^*P < 0.03$ compared with 0 ng/ml M-CSF in each group. Similar results were obtained from three independent experiments. **D:** H9c2 cardiomyocytes were incubated with reduced concentrations of PD98059 (6 μmol/L) or LY294002 (2 μmol/L). Left: H9c2 cardiomyocytes were treated with PD98059 or LY294002 for 30 minutes, stimulated with M-CSF (100 ng/ml) and inhibitors, and then analyzed as described in Figure 5. Right: H9c2 cardiomyocytes were treated with PD98059, LY294002, or without inhibitors (control) with (100 ng/ml) or without (0 ng/ml) M-CSF for 24 hours. Then the cells were stimulated with $H_2O_2$ (40 μmol/L) for 8 hours, and dead cells were assessed by WST assay. In each inhibitor group, dead cells at 0 ng/ml M-CSF are considered as 100%, and relative cell death rates at 100 to 0 ng/ml M-CSF in each inhibitor group are shown. $^*P < 0.02$ compared with 0 ng/ml M-CSF in each group.

abolished the protective effect of M-CSF (Figure 6C). LY294002 enhanced $H_2O_2$-induced cell death in H9c2 myotubes; however, M-CSF significantly protected H9c2 myotubes from cell death (Figure 6C). Moreover, a dose-response experiment of PD98059 or LY294002 was performed to observe ERK or Akt phosphorylation and cellular survival of H9c2 cardiomyocytes (Figure 6D). Similar results were obtained from H9c2 myotubes (data not shown). VEGF protected myogenic cells from cell death.[34] To confirm whether the cell survival effect of M-CSF de-

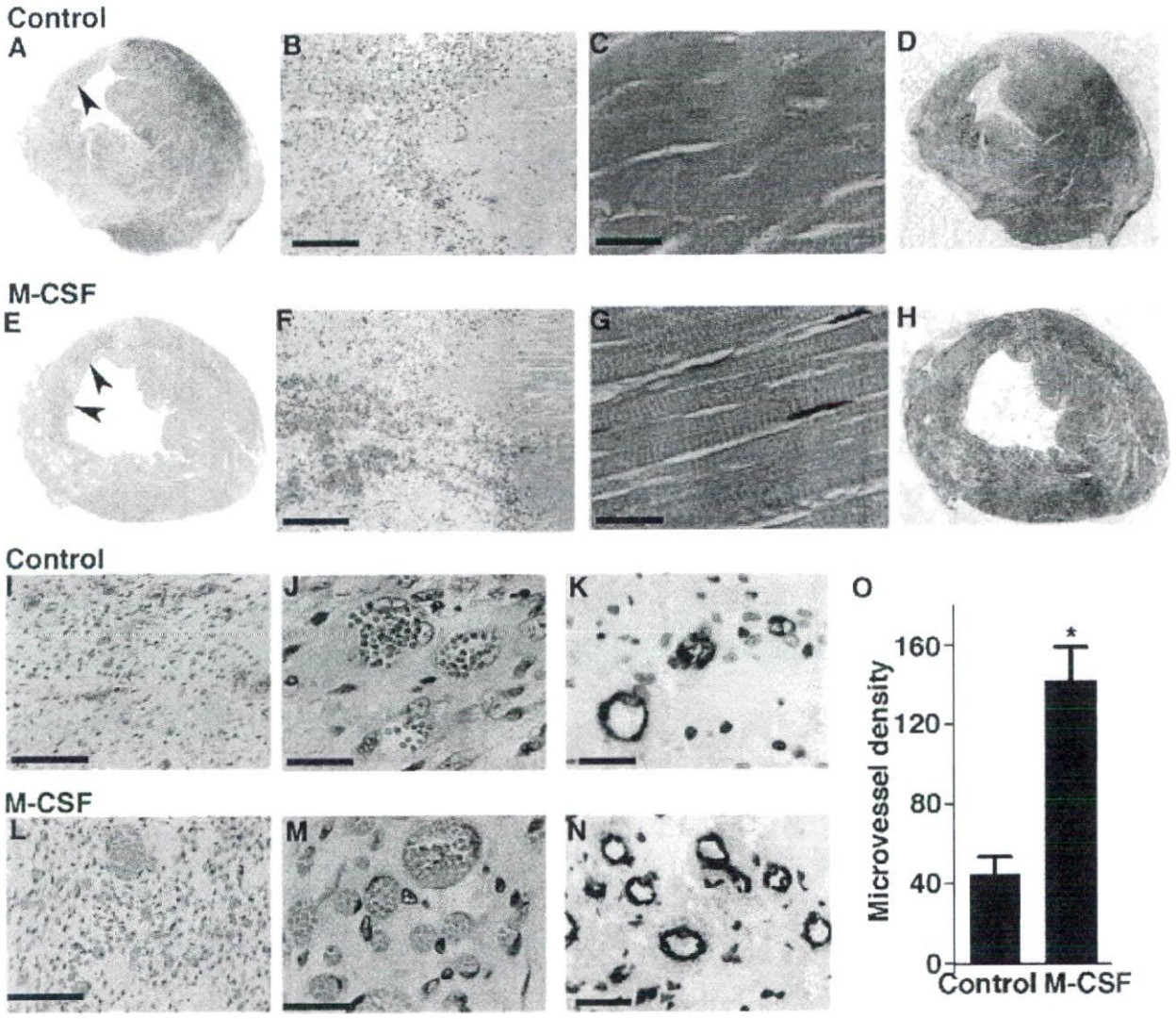


**Figure 7.** M-CSF promotes angiogenesis in goat heart after myocardial infarction. The goat left anterior descending coronary artery was permanently ligated, and the goats were sacrificed on day 14. M-CSF indicates goats intravenously injected with M-CSF shortly after the coronary artery ligation daily until day 13. Controls were injected with saline. Paraffin sections were stained with H&E (**A–C, E–G, I, J, L,** and **M**), Masson's elastic stain (**D** and **H**), and anti-factor VIII-related antigen antibody (**K** and **N**). **A** and **E:** Left anterior descending coronary artery ligation induced myocardial infarction. **Arrowheads** indicate cardiomyocytes in ischemic lesions. (**B, C, F,** and **G**) Microscopic observations indicated the cardiomyocytes in the ischemic lesions were dead. **D** and **H:** The green staining indicates fibrosis or scars in hearts. **I, J, L,** and **M:** The microvessels in ischemic lesions. **K** and **N:** The microvessels in ischemic lesions were immunohistochemically stained with anti-factor VIII-related antigen antibody. **O:** M-CSF significantly increased microvessel density in ischemic lesions ($^*P < 0.01$, $n = 3$ per group). The images represent one of three goats in each group. Scale bars: 200 μm (**B** and **F**); 20 μm (**C, G, J, K, M,** and **N**); 100 μm (**I** and **L**).

pends on VEGF, H9c2 cardiomyocytes and myotubes were cultured with an anti-VEGF antibody and M-CSF. Incubation with anti-VEGF antibody did not impair the cell protective effect of M-CSF from $H_2O_2$ stimulation suggesting that the effect of M-CSF was not VEGF-dependent (data not shown).

### *M-CSF Promotes Angiogenesis in Goat Ischemic Heart after Permanent Coronary Artery Ligation*

M-CSF treatment elevated systemic VEGF level in mice from a nondetectable level to potentially therapeutic levels.[14,15] The cell protective and angiogenic effects of M-CSF *in vivo* were examined using goats as a large animal model for myocardial infarction. Large animal models are necessary for evaluating growth factor-induced therapeutic angiogenesis,[3] and we have used goats for developing artificial heart devices.[27] We induced myocardial infarction by permanent left anterior descending coronary artery ligation. The coronary artery ligation resulted in LV infarction (Figure 7, A, D, E, and H). Macroscopically, M-CSF seemed to promote cardiomyocyte cell survival in ischemic lesions in comparison to the controls (Figure 7, A and E; arrowheads). Microscopy indicated that cardiomyocytes in ischemic lesions were dead cells in the controls (Figure 7, B and C). At low magnification, M-CSF seemed to protect cardiomyocytes from cell death in ischemic lesions (Figure 7F). However,

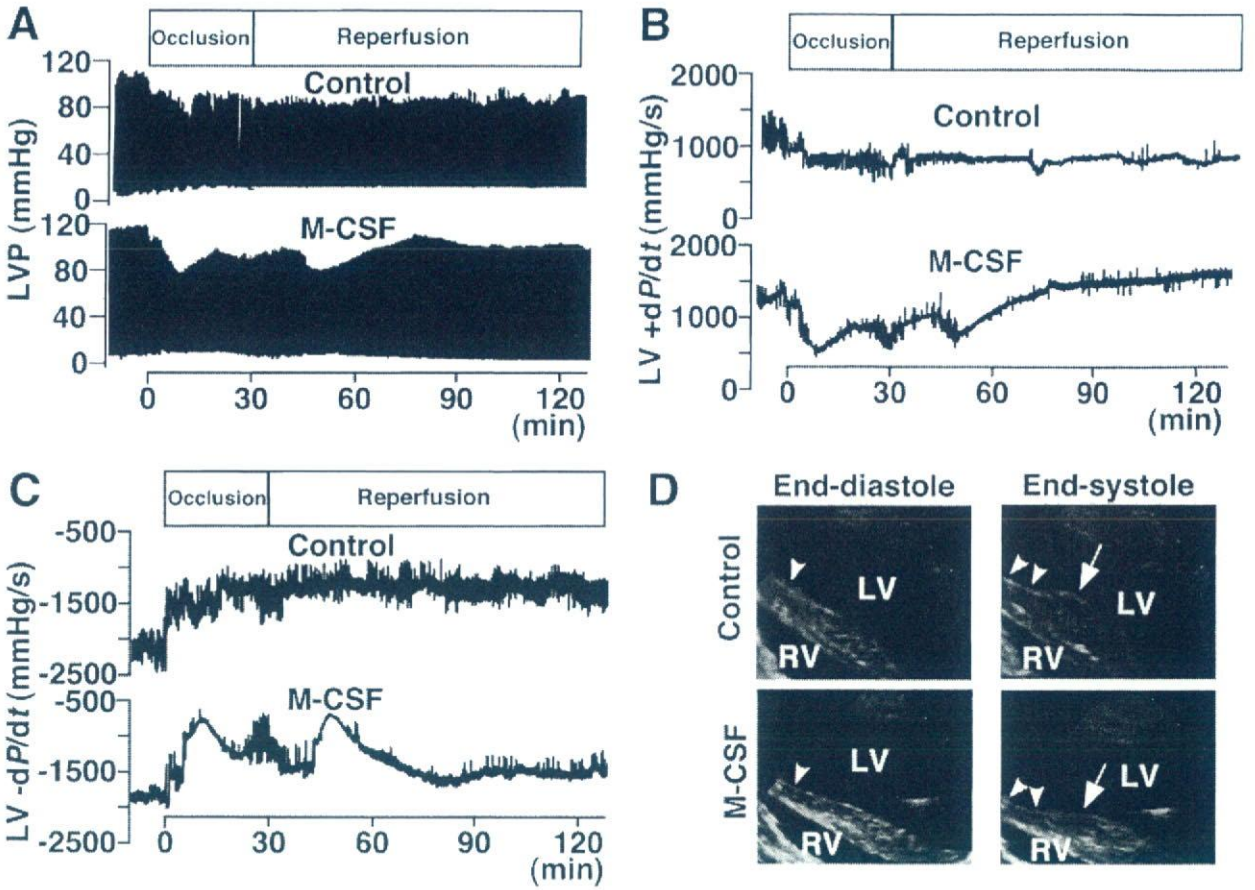


**Figure 8.** M-CSF pretreatment improved cardiac function after ischemic injury. M-CSF indicates goats intravenously injected with M-CSF daily for 3 days, whereas the control indicates goats injected with saline. The goat left anterior descending coronary artery was occluded for 30 minutes and then reperfused. **A–C:** Hemodynamic parameters before and during 30 minutes of left anterior descending coronary artery occlusion followed by 90 minutes of reperfusion are shown. Representative LVP records (**A**), representative positive dP/dt (**B**), and representative negative dP/dt (**C**) of control and M-CSF-treated goats. LVEDP, positive and negative dP/dt recovered in M-CSF-treated goats after reperfusion. **D: Arrowheads** indicate infarct areas. Compare **arrows**, which indicate wall contraction of nonischemic area at end systole, to **arrowheads**. In the infarct area, echocardiography shows dyskinetic wall movement in controls, whereas akinetic wall movement is shown in M-CSF-treated goats. Data are representative of three goats in each group.

at high magnification, most of the cardiomyocytes were dead (Figure 7G). Microvessels were observed in the ischemic lesions of control goats (Figure 7, I and J), and M-CSF treatment increased the number of microvessels (Figure 7, L and M). To confirm the microvessel density, we immunohistochemically stained goat hearts with anti-factor VIII-related antigen antibody (Figure 8, K and N).[23,24] M-CSF significantly increased microvessel density in ischemic lesions by 226% (Figure 7O). These results suggest that M-CSF promoted angiogenesis and induced collateral blood vessels in the ischemic heart. The infarct area quantification showed no significant difference between control and M-CSF-treated goats (controls, 30.4 ± 5.2%; M-CSF, 24.3 ± 2.1%). The residual presence of nuclei and cross striations in dead cardiomyocytes in ischemic lesions by M-CSF treatment (Figure 7G) suggests that the cardiomyocytes survived longer than control cardiomyocytes (Figure 7, C and G), but M-CSF-induced new vessels could not reach cardiomyocytes in ischemic lesions before their death.

### *M-CSF Pretreatment Improved Cardiac Function after Ischemic Injury Induced by Coronary Artery Occlusion-Reperfusion*

Erythropoietin treatment did not change the infarct size, but it improved cardiac function in the rat coronary artery occlusion-reperfusion model.[5] Pretreatment with stem cell factor and G-CSF improved cardiac function after myocardial infarction.[7] To confirm further the effects of M-CSF in myocardial infarction, goats were pretreated with M-CSF for 3 days, and then myocardial infarction was induced by 30-minute left anterior descending coronary artery occlusion followed by reperfusion.[5,35] Cardiac function was assessed by measuring hemodynamic parameters using catheterization analysis and examining echocardiography. Echocardiographic examination showed no significant differences in basal findings in cardiac function in both groups. Catheterization analysis showed the LV pressure (LVP) records of control and M-CSF-treated goats (Figure 8A). LV end diastolic pressure

(LVEDP), which can influence overall cardiac function,[4] increased after the left anterior descending coronary artery occlusion in both groups. In controls, the LVEDP did not recover after reperfusion, but in M-CSF-treated goats, the LVEDP gradually recovered after reperfusion (Figure 8A), and at 90 minutes after the reperfusion, the LVEDP of M-CSF treated goats was significantly better than that of control goats (controls, 10.62 ± 0.98 mmHg; M-CSF, 7.61 ± 0.83 mmHg; $P < 0.02$). Positive and negative dP/dt are measures of overall cardiac contractility and relaxation, respectively.[4] Positive dP/dt decreased after the left anterior descending coronary artery occlusion both in control and M-CSF-treated goats (Figure 8B). After reperfusion, positive dP/dt did not recover in control goats (Figure 8B). In M-CSF treated goats, positive dP/dt gradually recovered after reperfusion and finally reached similar dP/dt levels before the occlusion (Figure 8B). At 90 minutes after the reperfusion, the positive dP/dt of M-CSF-treated goats was significantly better than that of control goats (controls, 886 ± 103 mmHg; M-CSF, 1506 ± 125 mmHg; $P < 0.01$). Moreover, recovery of negative dP/dt after left anterior descending coronary artery occlusion-reperfusion was observed only in M-CSF-treated goats (Figure 8C). At 90 minutes after the reperfusion, the negative dP/dt of M-CSF-treated goats was significantly better than that of control goats (controls, −1342 ± 92 mmHg; M-CSF, −1570 ± 108 mmHg; $P < 0.05$). Echocardiographic examination showed a paradoxical LV wall movement area indicated as a dyskinetic area after left anterior descending coronary artery occlusion in control goats (Figure 8D). In M-CSF-treated goats, echocardiography showed a LV wall movement arrest area indicated as an akinetic area after left anterior descending coronary artery occlusion, and a dyskinetic area could not be found (Figure 8D). In control hearts, the nonischemic wall contractions at end systole were enhanced. This suggested substitutive wall movement for the dyskinetic area to keep cardiac output (Figure 8D). These echocardiographic findings suggest improvement of LV wall movement in M-CSF-treated goats during left anterior descending coronary artery occlusion-reperfusion. The LV ejection fraction (LVEF) was evaluated by echocardiography, but LVEF did not significantly change between before and after the occlusion; therefore, LVEF between controls and M-CSF-treated ones were not compared. Recovery of LVEDP, positive and negative dP/dt after reperfusion, and improvement of LV wall movement during the left anterior descending coronary artery occlusion-reperfusion suggest M-CSF pretreatment improved cardiac function after ischemic injury

## Discussion

In this study, M-CSF increased VEGF production in hearts both *in vivo* and *in vitro*. *In vitro*, M-CSF increased VEGF production through Akt activation. Moreover, M-CSF directly protected cardiomyocytes from cell death by activating Akt and ERK resulting in up-regulation of the downstream anti-apoptotic protein Bcl-xL. M-CSF-R expression in the heart was shown both *in vivo* and *in vitro*, and these results suggest that the expression is functional. Similar cell-protective effects of M-CSF on H9c2 myotubes were shown. *In vivo*, M-CSF treatment after the onset of myocardial infarction promoted angiogenesis in the ischemic heart, suggesting development of collateral blood vessels. Furthermore, M-CSF pretreatment in the goat myocardial infarction model improves cardiac function, as indicated by improvement of LVEDP, positive and negative dP/dt, and LV wall movements.

Recent studies indicate intramyocardial transfer of plasmid or adenoviral DNA-encoding human VEGF has favorable effects in myocardial infarction animal models and in patients with coronary artery diseases.[1,2,36] Similar to these VEGF transfer strategies, M-CSF directly up-regulated VEGF production in cardiomyocytes. In addition, M-CSF significantly induced an increase in plasma VEGF in mice to therapeutic levels that induced therapeutic angiogenesis.[14,35] Therapeutic plasmid gene delivery to a target organ is difficult and often temporary. However, M-CSF treatment was easily achieved by peripheral intravenous or intramuscular injection. These data indicate a therapeutic potential of M-CSF in ischemic heart diseases. Basic fibroblast growth factor and hepatocyte growth factor have also been applied to therapeutic angiogenesis.[37] We treated mice with M-CSF and examined basic fibroblast growth factor and hepatocyte growth factor mRNA levels by quantitative RT-PCR. M-CSF did not increase basic fibroblast growth factor or hepatocyte growth factor mRNA levels in the heart (data not shown). We also examined plasma G-CSF level after M-CSF treatment in mice by ELISA. M-CSF did not increase plasma G-CSF level. However, there is still a possibility that M-CSF induces other factors that are responsible for the effects shown in this article.

Very recently, M-CSF was reported to accelerate infarct repair and attenuate LV dysfunction in rats.[35] However, these authors did not investigate VEGF induction or the cardioprotective effects of M-CSF and did not use a large animal model. In the present study, in the M-CSF-treated group, we observed an increase in microvessel density, increased presence of dead cardiomyocytes, and decreased presence of granuloma in ischemic lesions. The increased presence of dead cardiomyocytes in ischemic lesions and improvement of cardiac function after ischemia in M-CSF-treated goats suggest a longer survival of cardiomyocytes in M-CSF-treated goats than in the controls. This finding and the decreased presence of granuloma suggest that M-CSF reduced the progression rate of ischemic injury in ischemic hearts *in vivo*.

In human monocytes, LY294002 suppressed M-CSF-induced ERK activation.[38] This mechanism was explained as M-CSF stimulation-induced reactive oxygen species, which activated ERK. The addition of Akt inhibitor prevented reactive oxygen species production and thus suppressed ERK activation in M-CSF-stimulated monocytes.[38] In murine myeloid cell line FDC-P1, LY294002 suppressed M-CSF-induced ERK activation, but it was not significant.[39] In H9c2 cardiomyocytes, LY294002 seemed to impair ERK activation in part. To suggest the involvement of Akt in M-CSF-induced ERK

activation in cardiomyocytes, we may have to use other Akt-inhibiting methods, as this time we could not reach a clear conclusion. For VEGF production, PD98059 treatment for 1 day did not affect M-CSF-induced VEGF production in differentiated H9c2 cells, whereas LY294002 treatment impaired M-CSF-induced VEGF production, suggesting M-CSF-induced VEGF production in differentiated H9c2 cells were Akt-dependent. This is the first report that suggested the presence of signal transduction pathways in cardiomyocytes in response to M-CSF. Further experiments are required for pursuing the M-CSF-induced intracellular signaling pathways in cardiomyocytes or in myotubes.

Goat hearts have a left coronary artery-dominant blood supply.[40] The goat coronary artery anatomy was remarkably regular, and coronary artery collaterals could not be demonstrated,[40] indicating frailty after heart ischemic injury. For the left anterior descending coronary artery occlusion-reperfusion model, the goat left anterior descending coronary artery was ligated at a point ~40% from the beginning of the left coronary artery to the apex, but LVEF decrease could not be detected by echocardiography. Occlusion of a more proximal site of goat left anterior descending coronary artery has been reported to be invariably fatal,[40] and our preliminary experiments with a more proximal left anterior descending coronary artery ligation supported this finding. Therefore, using goats, LVEF after myocardial infarction could not be evaluated. We were not able to assess plasma VEGF and the involvement of bone marrow-derived cells in the goat model because the appropriate reagents are not commercially available. We could not find a staining method specific for cardiomyocyte viability in goat hearts. Infarct area quantification suggested a trend that M-CSF might decrease infarct area. However, infarct area quantification showed no significant difference in control and M-CSF-treated goat hearts. Further investigation is required to clarify the roles and mechanisms of M-CSF in ischemic diseases using other species and other M-CSF treatment protocols.

The cell-protective and VEGF-inducing effects of M-CSF both in cardiomyocytes and myotubes were shown, and the effects were confirmed by improvement of cardiac function and activated angiogenesis in goat ischemic hearts. M-CSF is already in use clinically, and data from patients such as side effects are accumulating. Moreover, M-CSF administration is easily performed with minimal invasiveness in human patients. In this study, we showed the potential benefits of M-CSF treatment and its new mechanisms in ischemic heart diseases.

## Acknowledgments

We thank Peter Baluk, Hiroya Hashizume, Hiroshi Kubo, and Katsutoshi Nakayama for helpful comments on the manuscript; and Amy Ni and Shannon Freeman for correcting the manuscript.

## References

1. Yoon YS, Johnson IA, Park JS, Diaz L, Losordo DW: Therapeutic myocardial angiogenesis with vascular endothelial growth factors. Mol Cell Biochem 2004, 264:63–74
2. Kastrup J, Jorgensen E, Ruck A, Tagil K, Glogar D, Ruzyllo W, Botker HE, Dudek D, Drvota V, Hesse B, Thuesen L, Blomberg P, Gyongyosi M, Sylven C: Direct intramyocardial plasmid vascular endothelial growth factor-A165 gene therapy in patients with stable severe angina pectoris A randomized double-blind placebo-controlled study: the Euroinject One trial. J Am Coll Cardiol 2005, 45:982–988
3. Markkanen JE, Rissanen TT, Kivela A, Yla-Herttuala S: Growth factor-induced therapeutic angiogenesis and arteriogenesis in the heart-gene therapy. Cardiovasc Res 2005, 65:656–664
4. Parsa CJ, Matsumoto A, Kim J, Riel RU, Pascal LS, Walton GB, Thompson RB, Petrofski JA, Annex BH, Stamler JS, Koch WJ: A novel protective effect of erythropoietin in the infarcted heart. J Clin Invest 2003, 112:999–1007
5. Calvillo L, Latini R, Kajstura J, Leri A, Anversa P, Ghezzi P, Salio M, Cerami A, Brines M: Recombinant human erythropoietin protects the myocardium from ischemia-reperfusion injury and promotes beneficial remodeling. Proc Natl Acad Sci USA 2003, 100:4802–4806
6. Harada M, Qin Y, Takano H, Minamino T, Zou Y, Toko H, Ohtsuka M, Matsuura K, Sano M, Nishi J, Iwanaga K, Akazawa H, Kunieda T, Zhu W, Hasegawa H, Kunisada K, Nagai T, Nakaya H, Yamauchi-Takihara K, Komuro I: G-CSF prevents cardiac remodeling after myocardial infarction by activating the Jak-Stat pathway in cardiomyocytes. Nat Med 2005, 11:305–311
7. Orlic D, Kajstura J, Chimenti S, Limana F, Jakoniuk I, Quaini F, Nadal-Ginard B, Bodine DM, Leri A, Anversa P: Mobilized bone marrow cells repair the infarcted heart, improving function and survival. Proc Natl Acad Sci USA 2001, 98:10344–10349
8. Miki T, Miura T, Nishino Y, Yano T, Sakamoto J, Nakamura Y, Ichikawa Y, Ikeda Y, Kobayashi H, Ura N, Shimamoto K: Granulocyte colony stimulating factor/macrophage colony stimulating factor improves postinfarct ventricular function by suppression of border zone remodelling in rats. Clin Exp Pharmacol Physiol 2004, 31:873–882
9. Ohno R, Miyawaki S, Hatake K, Kuriyama K, Saito K, Kanamaru A, Kobayashi T, Kodera Y, Nishikawa K, Matsuda S, Yamada O, Omoto E, Takeyama H, Tsukuda K, Asou N, Tanimoto M, Shiozaki H, Tomonaga M, Masaoka T, Miura Y, Takaku F, Ohashi Y, Motoyoshi K: Human urinary macrophage colony-stimulating factor reduces the incidence and duration of febrile neutropenia and shortens the period required to finish three courses of intensive consolidation therapy in acute myeloid leukemia: a double-blind controlled study. J Clin Oncol 1997, 15:2954–2965
10. Kawakami Y, Nagai N, Ohama K, Zeki K, Yoshida Y, Kuroda E, Yamashita U: Macrophage-colony stimulating factor inhibits the growth of human ovarian cancer cells in vitro. Eur J Cancer 2000, 36:1991–1997
11. Stanley ER, Berg KL, Einstein DB, Lee PS, Pixley FJ, Wang Y, Yeung YG: Biology and action of colony-stimulating factor-1. Mol Reprod Dev 1997, 46:4–10
12. Giordano FJ, Gerber HP, Williams SP, VanBruggen N, Bunting S, Ruiz-Lozano P, Gu Y, Nath AK, Huang Y, Hickey R, Dalton N, Peterson KL, Ross Jr J, Chien KR, Ferrara N: A cardiac myocyte vascular endothelial growth factor paracrine pathway is required to maintain cardiac function. Proc Natl Acad Sci USA 2001, 98:5780–5785
13. Maharaj AS, Saint-Geniez M, Maldonado AE, D'Amore PA: Vascular endothelial growth factor localization in the adult. Am J Pathol 2006, 168:639–648
14. Okazaki T, Ebihara S, Takahashi H, Asada M, Kanda A, Sasaki H: Macrophage colony-stimulating factor induces vascular endothelial growth factor production in skeletal muscle and promotes tumor angiogenesis. J Immunol 2005, 174:7531–7538
15. Kalka C, Masuda H, Takahashi T, Gordon R, Tepper O, Gravereaux E, Pieczek A, Iwaguro H, Hayashi SI, Isner JM, Asahara T: Vascular endothelial growth factor$_{165}$ gene transfer augments circulating endothelial progenitor cells in human subjects. Circ Res 2000, 86:1198–1202
16. Kallies A, Rosenbauer F, Scheller M, Knobeloch KP, Horak I: Accumulation of c-Cbl and rapid termination of colony-stimulating factor 1 receptor signaling in interferon consensus sequence bind-

ing protein-deficient bone marrow-derived macrophages. Blood 2002, 99:3213–3219
17. Novak U, Harpur AG, Paradiso L, Kanagasundaram V, Jaworowski A, Wilks AF, Hamilton JA: Colony-stimulating factor 1-induced STAT1 and STAT3 activation is accompanied by phosphorylation of Tyk2 in macrophages and Tyk2 and JAK1 in fibroblasts. Blood 1995, 86:2948–2956
18. Kelley TW, Graham MM, Doseff AI, Pomerantz RW, Lau SM, Ostrowski MC, Franke TF, Marsh CB: Macrophage colony-stimulating factor promotes cell survival through Akt/protein kinase B. J Biol Chem 1999, 274:26393–26398
19. Ménard C, Pupier S, Mornet D, Kitzmann M, Nargeot J, Lory P: Modulation of L-type calcium channel expression during retinoic acid-induced differentiation of H9C2 cardiac cells. J Biol Chem 1999, 274:29063–29070
20. van den Eijnde SM, van den Hoff MJ, Reutelingsperger CP, van Heerde WL, Henfling ME, Vermeij-Keers C, Schutte B, Borgers M, Ramaekers FC: Transient expression of phosphatidylserine at cell-cell contact areas is required for myotube formation. J Cell Sci 2001, 114:3631–3642
21. Kang YJ, Zhou ZX, Wang GW, Buridi A, Klein JB: Suppression by metallothionein of doxorubicin-induced cardiomyocyte apoptosis through inhibition of p38 mitogen-activated protein kinases. J Biol Chem 2000, 275:13690–13698
22. Okazaki T, Sakon S, Sasazuki T, Sakurai H, Doi T, Yagita H, Okumura K, Nakano H: Phosphorylation of serine 276 is essential for p65 NF-κB subunit-dependent cellular responses. Biochem Biophys Res Commun 2003, 300:807–812
23. Seno H, Oshima M, Ishikawa TO, Oshima H, Takaku K, Chiba T, Narumiya S, Taketo MM: Cyclooxygenase 2- and prostaglandin $E_2$ receptor $EP_2$-dependent angiogenesis in $Apc^{\Delta 716}$ mouse intestinal polyps. Cancer Res 2002, 62:506–511
24. Bildfell RJ, Valentine BA, Whitney KM: Cutaneous vasoproliferative lesions in goats. Vet Pathol 2002, 39:273–277
25. Ebihara S, Guibinga GH, Gilbert R, Nalbantoglu J, Massie B, Karpati G, Petrof BJ: Differential effects of dystrophin and utrophin gene transfer in immunocompetent muscular dystrophy (mdx) mice. Physiol Genomics 2000, 3:133–144
26. Sakon S, Xue X, Takekawa M, Sasazuki T, Okazaki T, Kojima Y, Piao JH, Yagita H, Okumura K, Doi T, Nakano H: NF-κB inhibits TNF-induced accumulation of ROS that mediate prolonged MAPK activation and necrotic cell death. EMBO J 2003, 22:3898–3909
27. Wang Q, Yambe T, Shiraishi Y, Duan X, Nitta S, Tabayashi K, Umezu M: An artificial myocardium assist system: electrohydraulic ventricular actuation improves myocardial tissue perfusion in goats. Artif Organs 2004, 28:853–857
28. Kim WG, Cho SR, Sung SH, Park HJ: A chronic heart failure model by coronary artery ligation in the goat. Int J Artif Organs 2003, 26:929–934
29. Eubank TD, Galloway M, Montague CM, Waldman WJ, Marsh CB: M-CSF induces vascular endothelial growth factor production and angiogenic activity from human monocytes. J Immunol 2003, 171:2637–2643
30. Ide H, Seligson DB, Memarzadeh S, Xin L, Horvath S, Dubey P, Flick MB, Kacinski BM, Palotie A, Witte ON: Expression of colony-stimulating factor 1 receptor during prostate development and prostate cancer progression. Proc Natl Acad Sci USA 2002, 99:14404–14409
31. Baines CP, Molkentin JD: STRESS signaling pathways that modulate cardiac myocyte apoptosis. J Mol Cell Cardiol 2005, 38:47–62
32. Valks DM, Cook SA, Pham FH, Morrison PR, Clerk A, Sugden PH: Phenylephrine promotes phosphorylation of Bad in cardiac myocytes through the extracellular signal-regulated kinases 1/2 and protein kinase A. J Mol Cell Cardiol 2002, 34:749–763
33. Matsui T, Rosenzweig A: Convergent signal transduction pathways controlling cardiomyocyte survival and function: the role of PI 3-kinase and Akt. J Mol Cell Cardiol 2005, 38:63–71
34. Arsic N, Zacchigna S, Zentilin L, Ramirez-Correa G, Pattarini L, Salvi A, Sinagra G, Giacca M: Vascular endothelial growth factor stimulates skeletal muscle regeneration in vivo. Mol Ther 2004, 10:844–854
35. Yano T, Miura T, Whittaker P, Miki T, Sakamoto J, Nakamura Y, Ichikawa Y, Ikeda Y, Kobayashi H, Ohori K, Shimamoto K: Macrophage colony-stimulating factor treatment after myocardial infarction attenuates left ventricular dysfunction by accelerating infarct repair. J Am Coll Cardiol 2006, 47:626–634
36. Rutanen J, Rissanen TT, Markkanen JE, Gruchala M, Silvennoinen P, Kivela A, Hedman A, Hedman M, Heikura T, Orden MR, Stacker SA, Achen MG, Hartikainen J, Yla-Herttuala S: Adenoviral catheter-mediated intramyocardial gene transfer using the mature form of vascular endothelial growth factor-D induces transmural angiogenesis in porcine heart. Circulation 2004, 109:1029–1035
37. Azuma J, Taniyama Y, Takeya Y, Iekushi K, Aoki M, Dosaka N, Matsumoto K, Nakamura T, Ogihara T, Morishita R: Angiogenic and antifibrotic actions of hepatocyte growth factor improve cardiac dysfunction in porcine ischemic cardiomyopathy. Gene Ther 2006, 13:1206–1213
38. Bhatt NY, Kelley TW, Khramtsov VV, Wang Y, Lam GK, Clanton TL, Marsh CB: Macrophage-colony-stimulating factor-induced activation of extracellular-regulated kinase involves phosphatidylinositol 3-kinase and reactive oxygen species in human monocytes. J Immunol 2002, 169:6427–6434
39. Gobert Gosse S, Bourgin C, Liu WQ, Garbay C, Mouchiroud G: M-CSF stimulated differentiation requires persistent MEK activity and MAPK phosphorylation independent of Grb2-Sos association and phosphatidylinositol 3-kinase activity. Cell Signal 2005, 17:1352–1362
40. Lipovetsky G, Fenoglio JJ, Gieger M, Srinivasan MR, Dobelle WH: Coronary artery anatomy of the goat. Artif Organs 1983, 7:238–245

Proceedings of the 29th Annual International
Conference of the IEEE EMBS
Cité Internationale, Lyon, France
August 23-26, 2007.



# Quantitative Evaluation for Anastomotic Technique of Coronary Artery Bypass Grafting by using In-vitro Mock Circulatory System

Young Kwang Park, Yutaka Mita, Eriko Oki, Naohiko Kanemitsu, Yasuyuki Shiraishi, Yousuke Ishii, Takashi Azuma, Masami Ochi, and Mitsuo Umezu, *Member, IEEE*

*Abstract*—**This study focuses on the development of self-training system for surgical operation and quantitative evaluation of the surgical skills. Our group has developed a self-training system for anastomotic technique in Coronary Artery Bypass Grafting (CABG) to contribute the education of cardiovascular surgery without a risk to patients. The self-training system consists of following portions, 1) "YOUCAN", coronary and graft vascular silicone model, 2) "BEAT", a device, simulating stabilized myocardial surface, and 3) Quantitative evaluation system based on *in vitro* mock circulatory system. The coronary and graft model has been anastomosed by expert and trainee cardiac surgeon. The anastomosed model was mounted onto test section of the *in vitro* mock circulatory system then identical waveforms of coronary artery was applied into the inlet of an anastomosis. The energy loss was quantified as a pressure difference between proximal and distal ends of anastomosis. The energy loss was obtained as 67.3±1.75mJ (trainee) and 41.3±3.08mJ (registered surgeon). It was founded that average energy loss by expert surgeon was lower by 38.6% than that by trainee surgeon. The major difference among the models of expert and trainee was the Effective Orifice Area (EOA) of the anastomosis. Through the experiment, EOA was confirmed by image analysis as 2.73 mm$^2$ for an expert against 0.534 mm$^2$ for a trainee. In conclusion, it was suggested that the anastomotic skill among expert and trainee surgeons could be hydrodynamically differentiated by using *in vitro* mock circulatory system.**

## I. Introduction

ACCORDING to a statistical survey, there are 2,937 registered cardiac surgeons in Japan, whereas number of CABG cases was 20,095 in 2002 in Japan [1]. In other word, only 7 cases per one cardiac surgeon were performed in a year. The above data shows that situation is difficult to train trainee surgeons through the only clinical experience in operating theater. Training surgeons in a routine surgical operation is becoming difficult especially in a field of cardiovascular surgery from the view point of risks of medical safety for patients. To overcome the situation, alternative training program has been started in Japan. Fig.1 shows recently started surgical training program named WETLAB. Defrosted porcine hearts are installed into a simple cavity model. Registered surgeons closely teach surgical techniques to trainee surgeons. The advantages of the WETLAB are 1) understanding anatomy, 2) a real tactile feeling, and 3) no risk to patient. This training program is founded as effective and continually organized by major medical device companies under an indication of the academic society. Fig.2 shows the concept of staged surgical training system, which our group proposes. The DRYLAB stage has been set to complement the WETLAB stage. Artificial patient models and simulators are used instead of animal organs in the DRYLAB. The major difference of the both stages is that the DRYLAB provides self-training against the WETLAB provides group training. In fact, the WETLAB is effective training method, because the evaluation has been immediately done by supervisors. However, it is difficult to organize, daily. On the other hand,

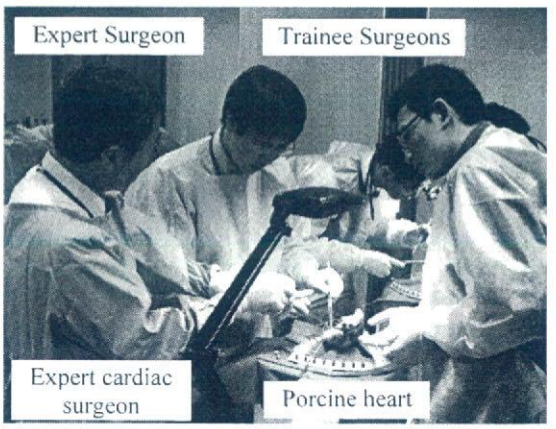


Fig.1. WETLAB in ordinary seminar room: Supervisor gives technical advice to trainee surgeons.

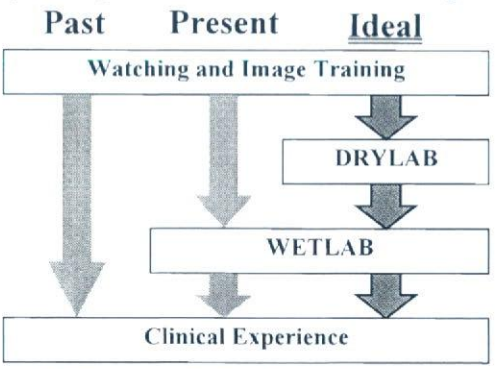


Fig.2. The concept of staged surgical training system.

This work was partly supported by "the robotic medical technology cluster in Gifu prefecture", Knowledge Cluster Initiative, Ministry of Education, Culture, Sports, Science and Technology, Japan, and also partly supported by the 21st Century Center of Excellence (COE) Program "The innovative research on symbiosis technologies for human and robots in the elderly dominated society", Waseda University, Tokyo, Japan

Y. Park is affiliated with Major in Integrative Bioscience and Biomedical Engineering, Graduate School of Waseda University, 58-322, 3-4-1 Ohkubo, Shinjuku-ku, Tokyo, Japan
(corresponding author to provide phone +81-3-5286-3256, fax +81-3-3200-2516, e-mail youngpark@moegi.waseda.jp)

1-4244-0788-5/07/$20.00 ©2007 IEEE